Chemical Process Design Vol.5 No.1 (2026) 62-86

University of Sistan and Baluchestan

Chemical Process Design

Available online at http://cpd.usb.ac.ir/

Comprehensive Evaluation of Side-Absorber Distillation Column Performance in Ethanol Extractive Dehydration

Aylin Dastouri[1], Behrooz Mahmoodzadeh Vaziri[1,2]✉

[1]Department of Chemical Engineering, Qu.C., Islamic Azad University, Quchan, Iran. Email: ailin.dastouri@yahoo.com
[2]Corresponding Author, Department of Chemical Engineering, Ma.C., Islamic Azad University, Mashhad, Iran.
Email: behrooz.vaziri@iau.ac.ir

ARTICLE INFO

Article type:
Research Article

Article history:
Received: 2025-07-12
Received in revised form: 2025-12-05
Accepted: 2025-12-05
Available online: 2025-12-05

Keywords:
Ethanol extractive dehydration; Side-Absorber Distillation; Model simulation; Sensitivity analysis; Optimization

ABSTRACT

A side-absorber distillation column (SADC) model was used for ethanol extractive dehydration (EED) with ethylene glycol (EG) as the solvent for the first time. The model performance was evaluated in terms of product purity, energy consumption rate, and the amount of solvent used. Initially, the system behavior was analyzed from a thermodynamic point of view. Then, the process was simulated, and the effect of all operational and design variables was separately and simultaneously evaluated through sensitivity analysis. By determining the optimal value of each variable, the SADC model was optimized. Using the optimized structure, ethanol with a molar purity of 99.8% and a specific energy consumption rate of 0.325 kWh/kg was extracted. Then, the performance of the SADC structure was operationally compared with classical two-column (CTC) and dividing wall column (DWC) configurations. In addition to maintaining high purity, the SADC model can reduce the reboiler heat duty by 37% and 30%, respectively, compared to the CTC and DWC structures. The amount of solvent consumed in the SADC structure was also reduced by 26.3% compared to the other two configurations. On the other hand, the SADC model is simpler and structurally smaller than other models, and it imposes less investment and operational costs.

Cite this article: Dastouri, A., Mahmoodzadeh Vaziri, B., (2026), Comprehensive Evaluation of Side-Absorber Distillation Column Performance in Ethanol Extractive Dehydration, *Chemical Process Design*, 5(1), 62-86. http//doi.org/10.22111/cpd.2025.52586.1065

Publisher: University of Sistan and Baluchestan.

DOI: http//doi.org/10.22111/cpd.2025.52586.1065

1. Introduction

Today, renewable energy sources have been identified as an appropriate solution to address concerns about the shortage of fossil fuels and the reduction of environmental pollution. Meanwhile, biofuels are considered one of the

best ways to replace conventional oil-derived fuels [1-3]. Biodiesel, renewable diesel, biogas (also known as biomethane), methanol, hydrogen, and bioethanol are examples of alternative biofuels. Biodiesel and renewable diesel are suitable alternatives to fossil diesel in compression ignition (diesel) engines. Biodiesel can exhibit cold flow and stability issues and may slightly increase NOx levels in engines. Biomethane offers great potential for CO_2 reduction but requires new storage and distribution infrastructure. Methanol has high octane but is corrosive. It has less energy per unit mass than gasoline and requires blending compatibility modifications. Hydrogen has very little volumetric energy unless it is liquefied or compressed. It can be used in fuel cells or burned in internal combustion engines (ICE). Fuel cells require completely different power transmission systems. H_2 could lead to very low carbon emissions, but its storage (350 to 700 bar or cryogenic) is a major limitation. Bioethanol, a sustainable and renewable biofuel, is clean and environmentally friendly, with broad blending compatibility. It produces fewer greenhouse gas emissions than petrol but with the same energy potential [4-6]. The major advantage of bioethanol compared to other alternative fuels is that it can be easily used in the existing fuel systems blended with gasoline (5-85%) without the need for modification of current engines and improved gasoline octane number index [3-5].

Ethanol can be produced commercially either through ethylene catalytic hydration or by fermentation of sugars. In order to use ethanol in gasohol, only ethanol with very low water content is allowed to prevent the malfunctioning of gasoline engines [7,8]. Therefore, an appropriate dehydration system is needed to produce anhydrous ethanol [7]. On the other hand, ethanol and water are an azeotropic mixture, the separation of which with the desired purity through conventional distillation is not possible [9,10]. As a result, high-purity ethanol needs special separation methods [8]. Among the most commonly used separation methods in ethanol dehydration are heterogeneous azeotropic distillation, extractive distillation (ED), pressure swing distillation, liquid-liquid extraction, surface absorption by molecular sieves, and the use of evaporative membranes [4-6,11-15]. The comparison between these separation methods in the ethanol dehydration process is given in Table 1.

Table 1. Comparison between separation methods in the ethanol dehydration process [5,6,14,15]

Metric	Molecular sieve	Pervaporation (membrane)	Azeotropic distillation (entrainer)
Typical product purity	≥99.5wt.% ethanol; ppm H_2O possible	Can reach ≥99.5 wt.% ethanol in retentate or via hybrid designs; flux drops at low feed water	Can achieve ≥99.5 wt.% ethanol but needs solvent recovery and decanting; trace entrainer removal required
Energy (thermal)	Moderate, regeneration steam/purge; good plant integration	Potentially lower thermal duty (if high flux membranes & heat-integrated) but needs vacuum/pumps	Often higher (reboiler duty for solvent recycle); solvent losses add effective energy/cost
Scalability	Very good (industry standard).	Good, but requires many modules at a very large scale	Good, conventional distillation scales easily
Feed sensitivity/fouling	Moderate, sensitive to contaminants; pre-distillation needed	High, membranes sensitive to fouling; pretreatment required	Low-moderate
Environmental/safety	Low (solid sorbent, limited toxic solvents)	Low-moderate (membrane waste, permeate handling)	Higher if toxic entrainers are used; solvent VOCs & losses

Despite the recent advancements in pervaporation membrane processes and surface absorption by molecular sieves, bioethanol is still massively produced by heterogeneous and extractive azeotropic distillation methods [3,4,14]. In both distillation processes, a third component called a separation agent, entrainer, or solvent, is added to the system, which modifies the liquid-vapor equilibrium behavior and improves the separation in the distillation column [1,9,10,14].

If the added entrainer generates a new azeotrope and a liquid-liquid biphasic system, the corresponding separation process is heterogeneous azeotropic distillation, which is widely used in ethanol dehydration [2]. The application of this process is accompanied by special complexities such as the formation of azeotropes and additional distillation boundaries, heterogeneous liquid-liquid equilibrium, a high degree of non-linearity, long-term instability, and multiple stable modes. These problems cause design, operational, and control challenges [2,16]. These complexities are not observed in ED, which, with the addition of a high-boiling point entrainer, is soluble without the generation of a new azeotrope accompanied by feed components [11,16,17]. In ED, the entrainer has a different interaction effect with each of the azeotropic components and shows a strong dependence on one of these key components [2,14,16]. This separation factor changes the coefficients of liquid phase activity and the relative volatility of the key components, thereby breaking the azeotrope [5,16-18].

The entrainers used in the EED process include organic solvents, solid salts (dissolved salts), hyperbranched polymers, ionic liquids (ILs) [8], and low-transition-temperature mixtures (LTTMs). Among these, organic solvents such as glycols and glycerol are recognized as the most commonly used entrainers in this industry [13,18]. In this paper, ethylene glycol (EG) has been used due to some benefits, such as high selectivity, and based on studies that indicate this solvent is most desirable for this process [9,11,12]. However, from an environmental point of view, the use and recovery of EG in distillation processes should be accompanied by some considerations. EG is biodegradable but toxic to aquatic life and mammals at moderate concentrations, so leaks, spills, or improper wastewater discharge can contaminate surface and groundwater. During recovery or regeneration by distillation, energy-intensive reboiling steps may increase greenhouse gas emissions if fossil-based heat sources are used. Volatilization losses are typically low due to EG's high boiling point, but degraded by-products (e.g., aldehydes, organic acids) may form under high-temperature conditions, contributing to air or water pollution if not captured. Overall, efficient heat integration, vapor recovery, closed-loop solvent recycling, and effective wastewater treatment are essential to minimize the ecological footprint of EG use in distillation systems [19,20]. The higher the selectivity of the entrainer, the lower the reflux ratio, and in turn, a smaller boilup ratio is required. Thus, the entrainer has a great impact on energy consumption [7,8,18]. In addition, high selectivity due to increased relative volatility leads to a reduction in the number of separation stages [18].

ED has been used extensively in various processes; however, the major drawback remains relatively high energy costs. [3,16]. An innovative solution to this problem is the use of advanced integration and intensification techniques, such as the use of heat-integrated columns and dividing wall columns (DWCs). Although the mentioned techniques are energy efficient, they each have their own defects. For example, heat-integrated ED systems require high investment costs, and DWCs are not widely used in the industry due to their design and control complexities [16]. The question that arises here is: What kind of extractive dehydration system can be more energy efficient?

In the present study, based on the principles of process integration and intensification, we attempted to answer this question by using an applicable structure to reduce the investment and energy costs of the EED process. In the next section, different ethanol dehydration structures are examined along with the proposed structure.

1.1. Ethanol extractive dehydration structures

The goal of all EED scenarios is to obtain high-purity products with minimal energy and solvent consumption. Hence, by presenting any model through which this goal can be attained, it can be claimed that a new method for ethanol

dehydration has been devised. In general, various structures of water-ethanol mixture extractive separation can be divided into three major categories: old, classical, and modern structures**.**

In the old methods, high energy consumption did not result in high-purity products, and usually, separation was continued to the azeotropic point. In these methods, the single-column structure was often used for separation. The most commonly used EED method is the use of the classic two-column (CTC) structure, where the first column is the extractive column and the second is the solvent recovery column. As shown in Fig. 1 (top-left), the entrainer (solvent) and feed are fed into the first column (azeotropic column) from the upper and middle trays, respectively.

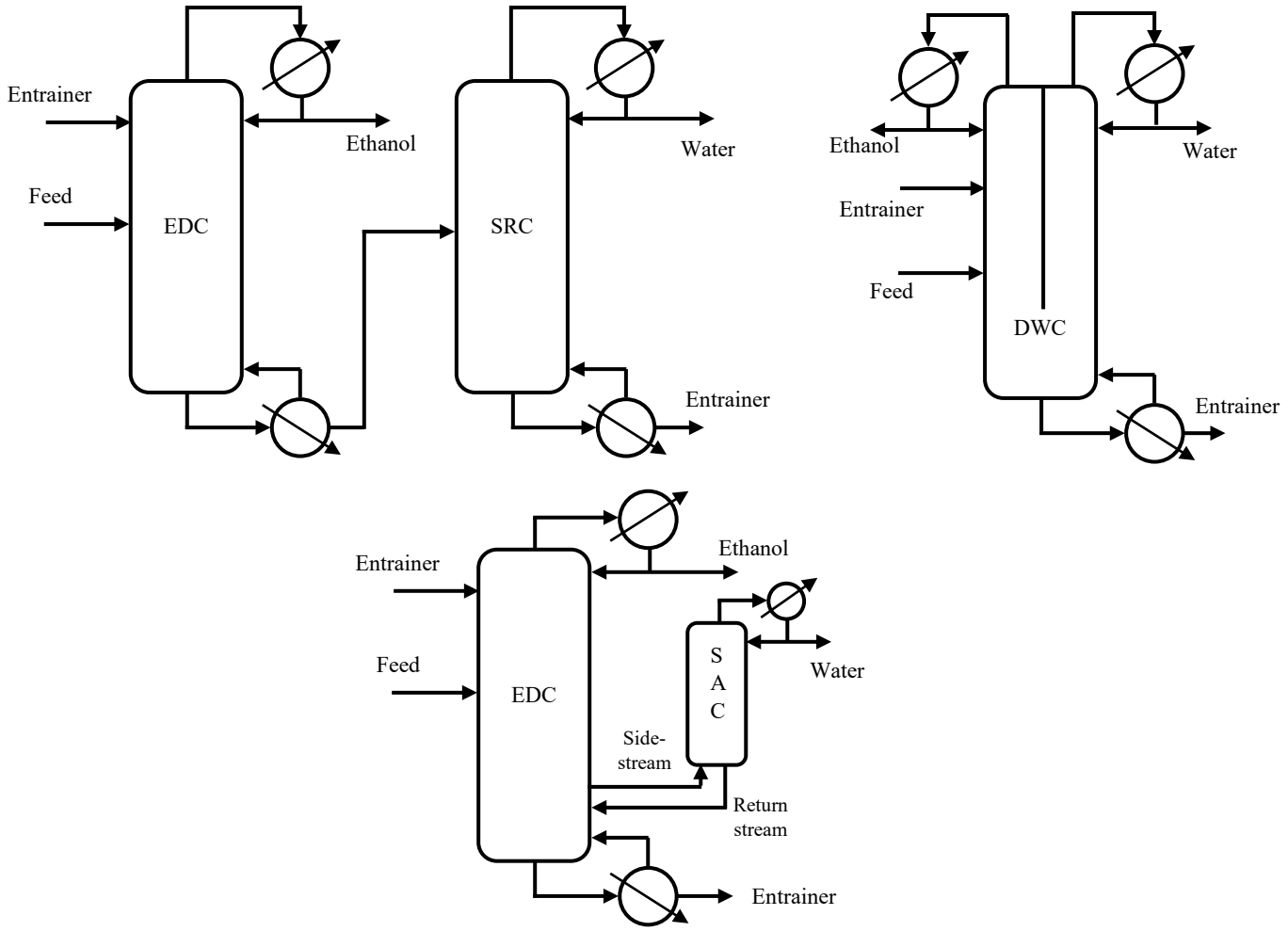

Fig. 1. Ethanol extractive dehydration structures: classic two-column structure (top-left), dividing-wall column structure (top-right), the proposed side-absorber distillation column structure (bottom)

The solvent changes the relative volatility of ethanol and water, such that separation becomes possible. Solvent is extracted by separating water from the bottom of the tower, and ethanol is extracted from the top of the column as a distillate product. Then, a mixture of solvent and water, which is a zeotropic mixture, is sent to the second column, and the solvent recovery operation is carried out. In this tower, the product is distilled water, and the solvent is removed from the bottom of the column and returned to the first column for reuse [2,3,7,10,12,14,18,21-23]. The classic structure, with two consecutive columns with four condensers and a reboiler, requires relatively high investment and operating costs. These factors have made ethanol purification on an industrial scale challenging in terms of funding and energy resources. Therefore, the replacement of new structures seems inevitable.

The use of DWCs shown in Fig. 1 (top-right) is introduced as one of these new methods. Solvent from the upper trays and feed from the middle trays enter the column. The solvent moves to the bottom of the column by separating water on the left side of the wall. Ethanol vapor flows upwards and is drawn off from the top of the column as a distillate from the left side of the wall. On the right side of the wall, water is separated from the solvent, and water is obtained as the distillate on the right side of the wall at the top of the column. Solvent recovery occurs at the bottom of the column, and the solvent is removed from the bottom of the distillation column [3, 21,24]. The relatively high price of DWCs, their design and difficulty in controlling them on the one hand, and the high global demand for ethanol on the other, necessitate the use of more state-of-the-art solutions.

To overcome these obstacles, this paper presents an alternative structural approach. The proposed structure is formed from a side-absorber distillation column (SADC) (Fig. 1-bottom). In this model, an extractive distillation column (EDC) was first used to mix the feed with the solvent and separate one of the key components of the feed (ethanol). Then, a side absorber column (SAC) was used to separate the second key component (water) from the solvent. The input feed into the SAC is received as a side stream from the EDC. The solvent (ethylene glycol (EG)) enters from the top trays of EDC, and after mixing with the feed stream, it binds with the existing water and ethanol and flows toward the final trays.

The hydrogen bond formed between EG and water is stronger than its bond with ethanol, so the solubility of water inside EG is more than the solubility of ethanol inside EG. Accordingly, as an appropriate extractor, EG can separate water from ethanol and take it down to the bottom of the column. By increasing the temperature in the lower parts of the EDC, the bond between EG and ethanol is broken, and ethanol is almost completely separated from the liquid mixture and moves through the vapor flow towards the top trays of the column. The passing vapor flow in the column is condensed after passing through the condenser, and high-purity ethanol is obtained. On the other hand, the flow of EG and water enters the reboiler, and it is heated up to bubble point temperature, and EG is heated until almost all the water is removed from the EG. Almost pure EG is obtained from the bottom of the column and again returned to the EDC as a solvent. To separate water from inside the tower, a side stream from the vapor phase is taken from the intake feed tray. Almost all the water, along with some EG and a small amount of ethanol, is taken out from the column and entered again as feed from the bottom of the SAC for water purification. This small column does not have a reboiler, and the side stream taken from the EDC acts as the supplier of the vapor phase in the absorption column. The inlet flow into the absorption column is in contact with the liquid reflux flow of the condenser and causes the EG in the vapor phase to be absorbed into the liquid phase. In this case, the vapor flow moves upwards, free of EG. This vapor flow is absorbed into the column condenser and condensed, and the high-purity water is obtained as the distilled product. The output flow from the EG-rich SAC floor is returned to a tray below the side stream tray to the EDC.

It should be noted that in the pre-concentration stage, the diluted ethanol stream (5 wt.%, 2 mol.%) obtained from the fermentation process is usually distilled in a distillation column typically to a near-azeotropic composition (93.5 wt.%, 85 mol.%) [3]. The pre-concentration stage is outside the scope of this article because the conventional distillation process is relatively obvious. In the next section, we have highlighted some of the most important studies in the field of ethanol dehydration that have used different separation models with an emphasis on the ED method.

1.2. Literature review

The presence of water inside ethanol is considered an impurity and reduces its solubility and fuel value. Therefore, ethanol dehydration has always been a concern for many researchers in order to achieve pure ethanol.

Alvarez et al. [12] in 2009 simulated and optimized the performance of EG and ionic liquid of 1-methyl-3-methylimidazolium dimethyl phosphate as a separation agent in the ED process. They studied the classic two-column and three-column structures to produce anhydrous ethanol from dilute solutions (11% by weight). The simulation results showed that both separation agents provide the same reboiler thermal loads to produce high-purity ethanol.

de Figueiredo et al. [10] in 2011 proposed a systematic method to determine the optimal conditions for the EED process using EG in classical structures without the need for multiple simulations. Solvent and distillate flow rates were introduced as the most effective factors in separation and energy consumption. The authors reported that the flow rate of the ethanol existing in the feed is the most suitable amount for the distillate flow rate.

Kiss and Suszwalak [3] in 2012 studied the process of ethanol dehydration through extractive distillation in DWCs with CTC structure using EG as the entrainer. They stated that the use of DWCs could save energy by over 10% relative to the classic model.

Gil et al. [2] in 2012 simulated and controlled the process of ethanol dehydration using the ED method and glycerol solvent in the CTC structure. They ascribed that the reflux ratio of EDC had the greatest impact on energy consumption; thus, this variable should be set to low values. Also, by varying the molar ratio of entrainer to feed, variations in some operating conditions can be compensated without affecting the amount of energy consumption.

In 2012, Alcántara-Avila [25] investigated distillation structures, entrainers, and energy saving methods to optimize the total annual cost, but the authors did not consider distillation columns with side absorbers.

Vazquez-Ojeda et al. [4] in 2013 designed and optimized the EED process by using the EG solvent. In their article, a comparison was made between the classic separation sequence along with the pre-concentration column and another configuration consisting of a classical structure along with a liquid-liquid extractor. For different concentrations of azeotropic feed, economic evaluation was performed on the two models. The results suggested significant savings in the annual cost by the proposed arrangement, when the ethanol content in the feed flow exceeds 10 mol.% (22 wt.%).

In 2013, Shirsat et al. [26] simulated and optimized EDC with pre-separators in the process of ethanol dehydration by using butyl propionate. The results showed higher separation efficiency and lower costs in the proposed process compared to the distillation method using pressure swings.

Kiss et al. [11] in 2014 used the CTC structure along with a preconcentration distillation column for the extractive dehydration of ethanol by EG solvent. In this study, the percentage composition of the distillate in the pre-concentration column (pre-concentrated ethanol) is presented as an important design variable. They investigated the effect of this variable on the annual costs of the whole process. Finally, the optimal concentration of this variable was reported as 91 wt.% (~ 80 mol.%) ethanol.

In May 2014, Quijada-Maldonado et al. [18] analyzed the mass transfer efficiency in ED for the ethanol dehydration using ionic liquids and EG. Simulations on the CTC structure were performed using sieve deck tray and Mellapak®250Y fillers in two proportions of solvent to feed. The results indicated the limiting effect of the relatively high viscosity of the column on the mass transfer coefficients. However, improvement in the relative volatility derived from ionic liquids helps to eliminate this effect. Nevertheless, it is not possible to solve this problem with very viscous solvents (>65 mPa.s at T=353.15K). They report that with the use of ionic liquids, the mass transfer efficiency increases with increasing the proportion of solvent to feed and reducing the proportion of distillate to feed.

Figueroa et al. [7] in 2015 showed that the use of ionic liquids as entrainers in the extractive separation of water and ethanol could provide high-purity ethanol with a recovery rate of more than 98%. In their study, ethanol with a purity of 76.69mol.% and a recovery rate of 99.39% was used in an optimized CTC model using 1-butyl-3-methylimidazolium dicyanamide ([bmim] [N(CN)2]) ionic liquid.

Zhu et al. [13] in 2016 investigated the feasibility of an ion-based ED process and determined the critical operating conditions for the production of anhydrous ethanol. Imidazolium ionic liquids were used as solvents. Simulations carried out on the CTC structure showed that ethanol with a purity of 99.9 mol.% is achievable.

García-Ventura et al. [24] in 2016 studied the production of high-purity ethanol through batch and continuous ED in DWC. They performed the dehydration process on feed containing 92 wt.% of ethanol. They stated that if glycerol is used as a carrier component in the extraction process, ethanol with a purity of higher than 99 wt.% could be extracted. This ethanol can be used in combination with gasoline to increase its function.

In 2017, Ma et al. [8] simulated ethanol dehydration under the ED process using low-transition temperature mixtures (LTTMs). Using a 3:1 glycolic acid-choline chloride (GC 3:1) as the entrainer, they improved the performance of EDC with a flash tank in terms of energy consumption.

Valentinyi et al. [22] in 2018 suggested process alternatives for the separation of a diluted ethanol–n-butanol–water mixture and simulated in the environment of ChemCAD® software. In their study, configurations of extractive (EG as an entrainer), heteroazeotropic distillation, and hybrid distillation-pervaporation systems for ethanol and n-butanol production were optimized based on the total annual costs. Ethanol and n-butanol were produced with a purity of 99.7 wt.% in all configurations. The results showed that the hybrid system should be applied for ethanol production, while n-butanol can be produced more economically with heteroazeotropic distillation.

Thein et al. [27] in 2018 carried out ethanol dehydration by the ED process. They used EG as an entrainer with calcium chloride as a salt to improve the purity of ethanol. Different ratios of ethanol-water and EG, such as (1:1:0, 1:1:0.25, 1:1:0.25 (salt=20 wt.% of solvent)) were analyzed to obtain the best ethanol purity. In their research, an ethanol concentration of 82 vol.% was obtained from the concentration of 52 vol.% ethanol in the feed mixture by a simple batch distillation approach. By an ED with EG, 88vol% ethanol was produced from 52vol% ethanol in the feed mixture. 92vol% ethanol was accomplished from 52vol% ethanol in the feed mixture by ED with dissolved salt (CaCl2) in the solvent.

Ramírez-Corona et al. [28] in 2019 explored the dynamic implications of the use of two types of ionic liquids on the ethanol-water ED system. These ionic liquids were 1-methylimidazolium chloride ([mim]Cl), and 1-butyl 3-methylimidazolium chloride ([bmim]Cl). Their analysis was conducted for different ionic liquid concentrations. Their results indicated that changing the ionic liquid concentration affects the degree of stabilization of the product stream. Furthermore, [mim]Cl offered good potential for its implementation as an entrainer for ethanol dehydration extractive columns.

Miranda et al. [14] in 2020 studied the performance of the extractive and azeotropic distillation processes in the CTC structure for anhydrous ethanol production, via simulation in the Aspen Plus™ environment. They applied EG and cyclohexane as solvents. In their work, anhydrous ethanol was obtained from the top of the 1st column of the ED (including 22 stages) with a purity of 99.50mol%, and water with 99.20mol% purity at the top of the 2nd column. In the azeotropic distillation, anhydrous ethanol in the bottom product of the 1st column (including 30 stages) had a purity of 99.99mol%, and water at the bottom of the 2nd column had a purity of 99.99mol%. Both processes produced

anhydrous ethanol with a high-grade purity. Based on their results, the ED spent 1,928.2 kW in the reboilers against 4,680.3 kW in the azeotropic distillation, indicating that ED is the most economical option. Finally, they pointed out that the ED is much more competitive than azeotropic distillation for this type of mixture, although azeotropic distillation yields a higher purity of anhydrous ethanol.

Guerrero-Martin et al. [23] in 2023 analyzed the exergy load distribution in ED for ethanol dehydration. The process simulation was carried out using Aspen Plus® software. They pointed out that heat transfer processes (heating or cooling) cause the most exegetic destruction and therefore need to be optimized. Based on their results, the local exergy efficiency of the CTC structure was 13.80%, which was the operation with the highest energy loss, and the overall exergy efficiency of the separation system was 30.67%.

It is noteworthy that almost all the papers on this topic have focused on CTC and DWC structures, in which no significant new achievements are observed. The aforementioned structures consume large amounts of solvent and energy and require high investment costs. The main goal of this research is to identify the optimal conditions for an alternative separation model that reduces the operational costs (energy duty and solvent use) and capital expenses of the EED process. The proposed model essentially implements the ED method in distillation columns with a side absorber. First, the thermodynamic behavior of the system, including process equilibrium, distillation boundaries, residue curves, and potential product regions, was analyzed. Using Aspen Plus® simulator (version 2019) and sensitivity analysis, the effects of all key parameters were examined both individually and collectively. By establishing the optimal ranges for each parameter, the model was optimized. Finally, the performance of the SADC model was compared to other models (CTC and DWC) based on product purity, design specifications, energy use, and solvent consumption. To the best of our knowledge, this is the first comprehensive assessment of the performance of columns with a side absorber in the EED process.

2. Process thermodynamics

The correct prediction of the thermodynamic behavior of the mixtures plays a key role in the simulation. Since distillation columns always have a balance between phases, it is very important to use thermodynamic equations that can predict the equilibrium properties of the system. For non-ideal mixtures such as water/ethanol/EG, activity models are used for thermodynamic analysis. According to previous studies, the EED process has been used more than the NRTL [2,3,8,10-14,17,18] and UNIQUAC [3,22,26] equations.

In this study, the performance of two models of physical properties of NRTL and UNIQUAC was evaluated to predict the thermodynamic behavior of the mixture and the non-ideality description of the liquid phase. The binary parameters of these models were taken from the Aspen Plus® database and were presented in Tables 2 and 3. The accuracy of the thermodynamic models used was verified by the laboratory equilibrium data extracted from the reference [29].

Table 2. Binary interaction coefficients for the NRTL model

Component i	Component j	Aij	Aji	Bij	Bji	Cij
H_2O	ETHANOL	3.4578	-0.8009	-586.0809	246.18	0.3
H_2O	EG	0.3479	-0.0567	34.8234	-147.1373	0.3
ETHANOL	EG	14.8422	-0.1115	-4664.4058	157.5937	0.47

Table 3. Binary interaction coefficients for the UNIQUAC model

Component i	Component j	Aij	Aji	Bij	Bji	Cij	Cji
H_2O	ETHANOL	-2.4936	2.0046	756.9477	-728.9705	0	0
H_2O	EG	-0.6018	0.6018	120.7787	-18.6714	0	0
ETHANOL	EG	-8.2308	2.6876	2632.9255	-959.5647	0	0

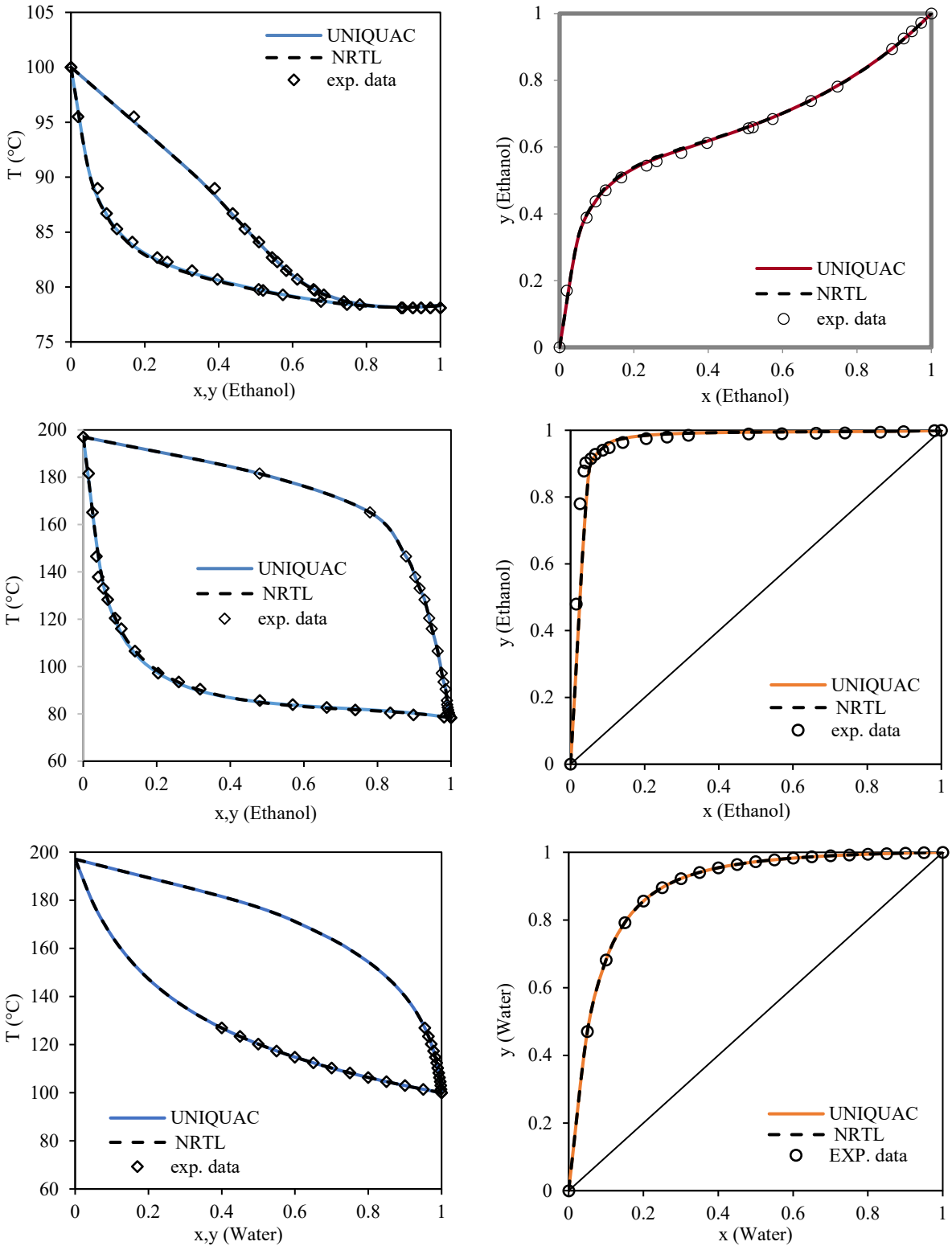

Fig. 2. T-xy and xy phase equilibrium diagrams; water/ethanol (top), ethanol/EG (middle), water/EG (bottom)

The xy and T-xy vapor-liquid equilibrium diagrams are shown in Fig. 2. According to the obtained results, the predictions obtained from the NRTL and UNIQUAC equations are the same in almost all cases and are highly in accordance with laboratory data. According to Fig. 2 (top), a mixture of water and ethanol at atmospheric pressure has a homogeneous azeotrope with a minimum boiling point of 15.88°C at a concentration of 89mol.% (95 wt.%) of ethanol. As a result, the components of this mixture cannot be separated in a conventional distillation column. If this mixture is fed to an atmospheric column, the purity of ethanol in the distillate will not exceed 89mol%. However,

high-purity water can be drawn off from the bottom of the column. It is clear from Fig. 2 (middle) that the difference between the ethanol molar fraction between the vapor and liquid phases in the xy diagram and the difference between the curves of the bubble and dew points in the T-xy diagram is very high. Under these conditions, the separation of ethanol from EG is easily accomplished without the need for a large number of equilibrium stages. As shown in Fig. 2 (bottom), the water/EG mixture does not have a fusion point at any temperature. Thus, this mixture is simply separable with the conventional distillation, such that if the molar fraction of water inside the liquid phase reaches from 0 to 0.3, the molar fraction of water inside the vapor phase reaches 0.9 from 0.

According to the results, both equations have excellent performance in the approximation of the equilibrium of binary systems. In the present study, the NRTL equation was used to predict the thermodynamic behavior of the mixture. The analysis of the remaining curves and the determination of the distillation boundaries and possible areas for receiving the column products were carried out using the NRTL model.

2.1. Ternary phase diagram and residue curves

Ternary phase diagrams with residual curves, distillation boundaries, and interface lines are excellent tools for identifying constraints in highly non-ideal systems. These diagrams can be introduced as a simple method for designing ED layouts [2, 13]. Therefore, before process simulation, it is necessary to identify the properties of the ternary system and the possibility of separation by using the solvent of interest. Then, according to the feed location, determine the zone of receiving the top and bottom products of the column. In Fig. 3, the ternary diagram and a map of residue curves of the water/ethanol/EG system at atmospheric pressure are plotted using Aspen Plus software.

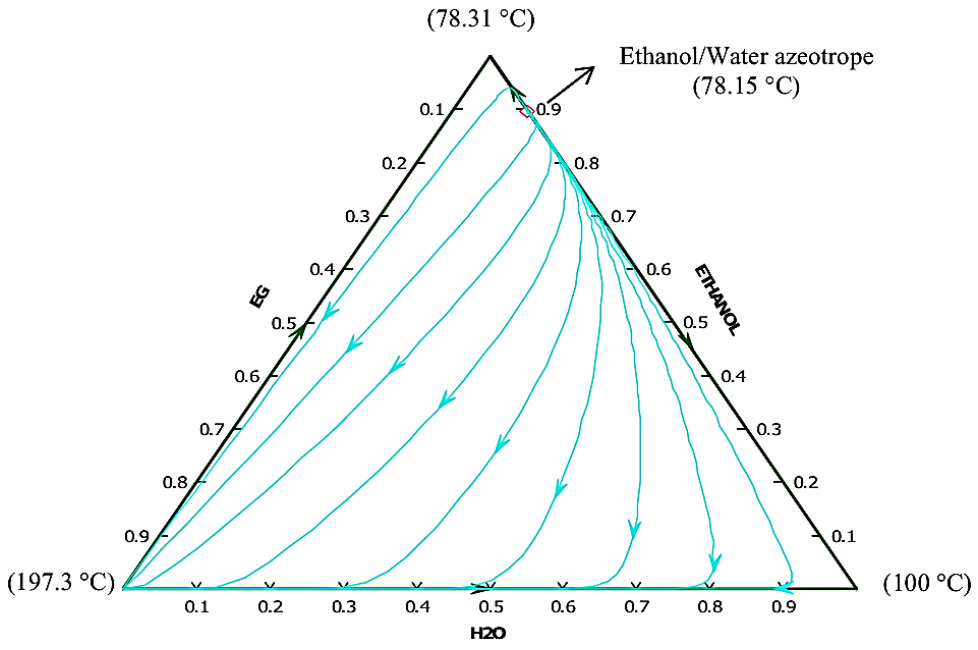

Fig. 3. Ternary phase diagram and residue curves of water/ethanol/EG mixture at 1 atm

Due to the solubility of all three components in each other, no phase changes are observed in the liquid mixture. The distillation boundaries correspond to the three sides of the triangle, and one distillation region is generally visible. This means that there is no boundary limit in the extraction of high-purity products. According to Fig. 3, out of the four nodes, three nodes belong to the pure components, and one node corresponds to the azeotrope point of water and ethanol. The lowest temperature belongs to this azeotrope and is known as an unstable node. On the opposite side,

EG has the highest boiling temperature and is subsequently referred to as a stable node. Pure water and ethanol at the other two vertices form the horse saddle nodes. As shown in Fig. 3, the residue curves start from the azeotropic point and end at EG after moving to the horse saddle nodes. Accordingly, it is expected that pure ethanol could be obtained from the top of the column, while the mixture of EG and water is drawn at the bottom of the EDC.

3. Process simulation

Technical and economic evaluations through process simulation are inevitable for the implementation of industrial-scale units. The SADC structure for the production of anhydrous ethanol was implemented and simulated using the ED method in the powerful Aspen Plus software environment (version 2019). The simulation flowsheet is shown in Fig. 4. EDC and SAC were modeled in the simulation process using RadFrac columns. Condensers and reboiler were modeled according to the total and Kettle type, respectively.

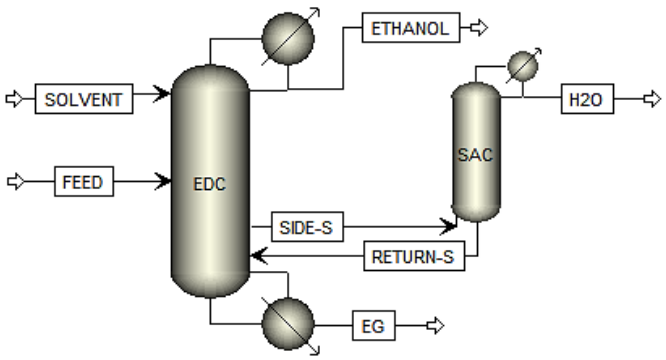

Fig. 4. SADC simulated flowsheet in Aspen Plus simulator

In order to make an accurate comparison between different separation structures, the feed and solvent conditions used were similar to those of Antoine Kiss et al. [3]. Here, the feed flow obtained from the preconcentration stage is bioethanol and has a composition near the azeotropic point (85mol.%, 93.5 wt.% ethanol). Table 4 presents the conditions for feed and solvent flows entering the EDC**.**

Table 4. The characteristics of the inlet streams to the EDC

Stream	Components	Temperature (°C)	Pressure (atm)	Flow rate (kmol/hr)
Feed	Ethanol	90	1	85
	Water	90	1	15
Solvent	EG	90	1	190

Since the azeotrope of the water and ethanol mixture was pressure dependent, the effect of pressure on the azeotrope point was analyzed, and the corresponding results were presented in Table 5. According to Table 5, by reducing the system pressure to 1 atm, a higher purity of ethanol can be achieved while reducing the boiling point of the mixture. For this reason, all simulations were performed at an operating pressure of 1 atm.

Table 5. The variations of the azeotrope point of the water/ethanol mixture with pressure

Pressure (atm)	Temperature (°C)	x (ethanol)
1	78.15	0.895
2.5	103.3	0.869
5	125.36	0.846
7.5	139.75	0.830
10	150.73	0.818

In Fig. 5, the average composition of the three-component mixture and the corresponding mass balance lines in the extractive distillation column and side absorber are presented in the ternary diagram. The EDC mass balance line starts from the EG node at the bottom of the column and extends toward the ethanol node at the top of the column. In the SAC, which has only one product, the mass balance line starts from the pure water node at the top of the column and moves to the side of ethanol/EG at the bottom of the column. On the basis of mass balance lines in the ternary diagram, the range of products received from the top and bottom of columns was determined, and simulations were made on this basis.

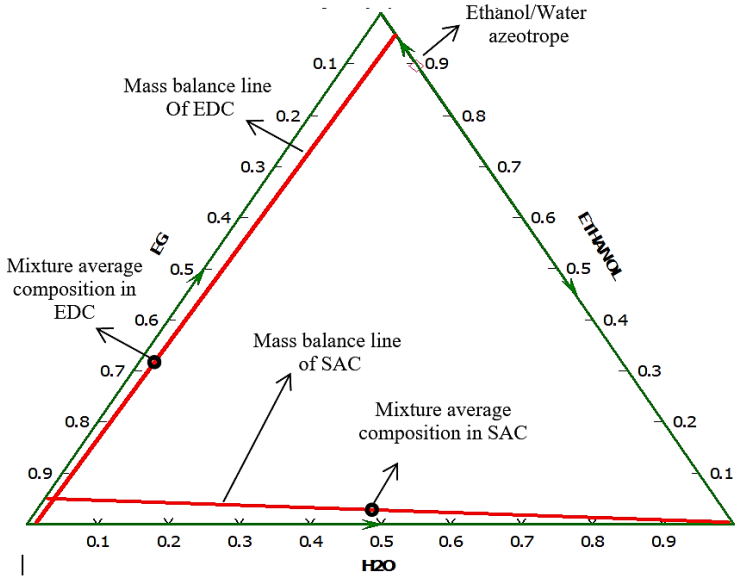

Fig. 5. The mass balance lines and the feed locations of EDC and SAC in the ternary diagram for the proposed structure

In Table 6, the specifications used in the initial simulation of the proposed model are presented, and the column hydraulics and simulation assumptions are given in Table 7. The results of the initial simulation are given in Table 8. The data used for the initial simulation in the Aspen Plus software environment were based on our knowledge and review of articles in this field. All simulations converged with mass and energy balance errors below 0.01%, and solver residual tolerance below 1×10^{-6}, indicating negligible numerical uncertainty. In all cases, the number of iterations was limited to a maximum of 100. The variations of the results in the final iterations were less than 0.1%, indicating the stability of the system.

Table 6. The specifications used in the primary simulation of the SADC model

The primary simulation parameters	Value	Unit of measurement
Number of EDC stages	25	-
Number of SAC stages	15	-
EDC reflux ratio	0.55	kmol/kmol
SAC reflux ratio	1.14	kmol/kmol
Feed stage in EDC	13	-
Solvent stage in EDC	3	
Drawing stage of the side stream from EDC	16	
Returning stage of the side stream to EDC	17	-
Side stream flow rate	30	kmol/hr
EDC distillate flow rate	85	kmol/hr
SAC distillate flow rate	15	kmol/hr

It should be noted that ethanol should have a minimum purity of 98.7mol.% (99.5 wt.%) to be used as raw material in chemical industries or as fuel in current engines [13]. The purity of other obtained products (water and EG) is also important for the purity of ethanol because of their reuse in the process. In the initial simulation, a purity above the standard value for ethanol was achieved. As a result, the only remaining action is to minimize the energy consumption of the process.

Table 7. Column hydraulics and simulation assumptions in the SADC model

Column hydraulics and specifications	Type or value
Tray	Sieve
Stage efficiency (%)	70 (for all components)
Total height (m)	12.2
Diameter (m)	0.84
Tray spacing (m)	0.6096
Number of passes	1
Hole diameter (m)	0.0127
Hole area/active area	0.1
Weir height (m)	0.508
Weir length (m)	0.609
Downcomer width (m)	0.131
Approach to Flood (%)	80

Table 8. Results of the initial simulation by the SADC model

Parameter	Value
Purity of the produced ethanol (mole fraction)	0.998
Purity of the produced water (mole fraction)	0.987
Purity of the produced EG (mole fraction)	0.999
Reboiler heat duty in EDC (kW)	1673.66
Condenser heat duty in EDC (kW)	-1439.59
Condenser heat duty in SAC (kW)	-365.81

Therefore, optimization of the model was performed using sensitivity analysis. Using the sensitivity analysis, the effects of continuous and discrete variables were investigated distinctly and simultaneously. By determining the optimal range of variables, an attempt was made to reduce energy consumption and even increase the purity of the received products. Then, the results of the SADC model were compared with the results of the CTC and DWC configurations presented in the articles. This comparison was based on specific criteria such as design specifications, product quality, and energy and solvent consumption.

4. Sensitivity analysis

One of the most important parts of any process is always finding the optimal value of the key parameters that affect the process. Using sensitivity analysis, we can investigate the effects of all factors affecting the system, including continuous and discrete factors, and determine the optimal amount or range of each of these factors. This can improve the performance of a structural model by reducing investment and operational costs. In the present study, we have tried to provide an optimal separation pattern to achieve high-purity products with the lowest energy and investment costs. Since the purity of recovered products in the initial simulation is acceptable, an attempt has been made to minimize the energy duty of the process by determining optimal design and operating parameters. Aspen Plus® Sensitivity Analysis Tool (version 2019) was used to optimize the process. Operational and design variables affecting product purity and energy consumption of the process can be divided into two groups of continuous (solvent rate, EDC reflux ratio, feed and solvent temperatures, and side stream flow rate) and discrete (number of EDC and SAC

stages, feed, solvent, and side stream stages). Studying the impact of all variables on a process simultaneously and over a wide range is very complex and difficult. As a result, the effect of each factor was first examined individually to determine its relatively optimal range. For this purpose, the value of a specified variable over a logical range was changed, while the value of other variables was kept constant. The major part of the operating costs of the distillation process is related to providing the energy required for the reboilers. Therefore, the effect of each variable, in addition to product purity, on the heat duty of this main source of energy consumption was investigated. After determining the optimal range of each variable, sensitivity analysis was simultaneously performed on all variables within their optimal range to determine the best operating and design conditions.

4.1. Effect of the solvent flow rate

Fig. 6 shows the effect of solvent flow rate changes on the purity of the products and the heat duty of the reboiler. Solvent flow rate plays a decisive role in the ED process because its increase, on the one hand, improves the purity of the products and, on the other hand, increases the energy consumption of the system.

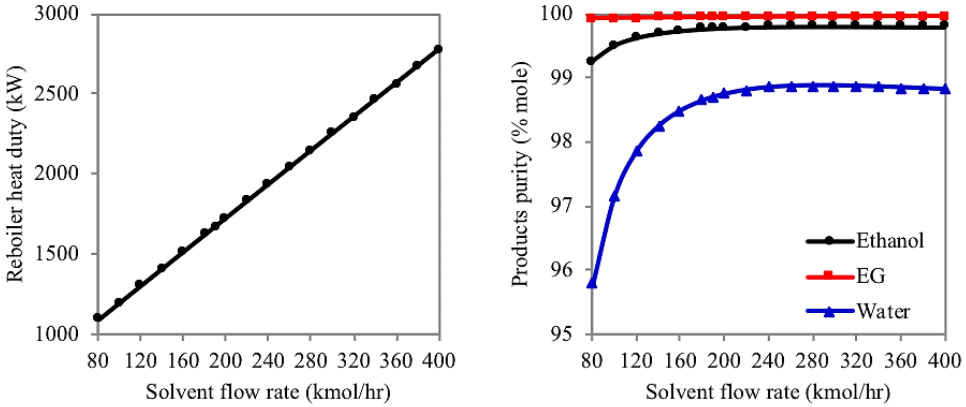

Fig. 6. The effect of solvent flow rate on the purity of the products (right) and reboiler heat duty (left)

It is clear from Fig. 6 (right) that increasing the solvent flow rate to a specified level increases the purity of ethanol and water. This increase in purity for ethanol is almost up to 180 kmol/hr solvent flow rate, and for water, to a solvent rate of 220 kmol/hr. However, the increase in solvent flow rate does not have much effect on the purity of recovered EG. On the other hand, by increasing the solvent flow rate from 80 to 400 kmol/hr, due to the rising flow rate of the reboiler, the unit's energy consumption increases linearly from about 1091 to 2774 kW (Fig. 6, left). As indicated in Fig. 6, the suitable range for solvent flow rate, to reduce energy consumption and obtain acceptable purity, was considered between 130 and 220 kmol/hr.

4.2. Effect of the number of EDC stages

The effect of varying the number of EDC stages on the purity of the products and the heat duty of the entire process is shown in Fig. 7. As shown in Fig. 7 (left), with increasing the number of equilibrium steps up to 21, the heat duty of the reboiler decreases sharply. Then, until stage 22, the descending trend continues with a mild gradient, and after that, it becomes almost constant. Since the number of stages in the studied range does not have a significant effect on the purity of the products (as shown in Fig. 7, right), the number of optimal stages can be 21 to 22 (according to Fig. 7, left).

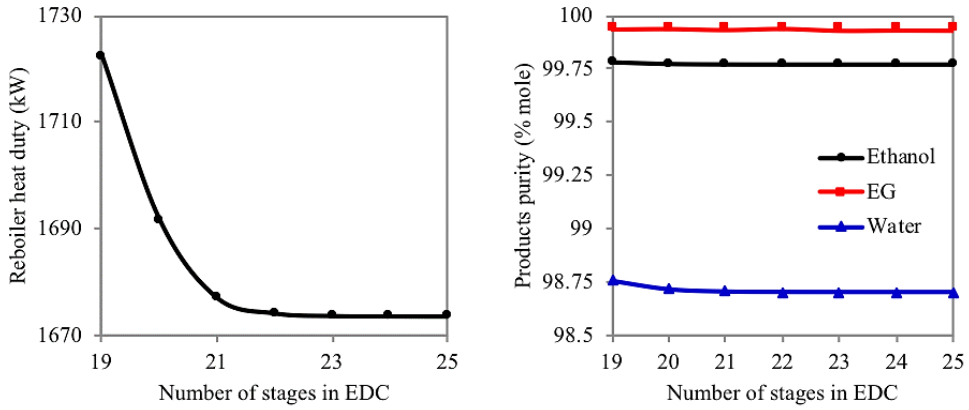

Fig. 7. The effect of the number of EDC stages on the purity of the products (right) and reboiler heat duty (left)

4.3. Effect of the number of SAC stages

Changing the number of SAC trays did not significantly affect the product purity and energy consumption rate of the proposed model. Because, as seen in the thermodynamics section of the process, water separation from EG in SAC is rapid and does not require a large number of stages. Therefore, the least number of equilibrium stages (4 stages) that leads to convergence of the simulation was considered for SAC**.**

4.4. Effect of the EDC reflux ratio

Fig. 8 shows the effect of changes in the EDC reflux flow ratio on the purity of the products and the heat load of the reboiler. Increasing the return flow ratio by increasing the circulating fluid flow inside the column increases the purity of the product and the amount of energy consumed by the unit. As shown in Fig. 8 (right), the purity of recovered products increases with a rise in the reflux flow to a specified limit, but then becomes steady. Therefore, to avoid increasing energy consumption (Fig. 8-left), non-use of high values of the reflux flow ratio is necessary. According to the results, to achieve high levels of purity on the one hand and minimum energy consumption on the other, the optimum range for the reflux flow ratio was 0.4-0.7.

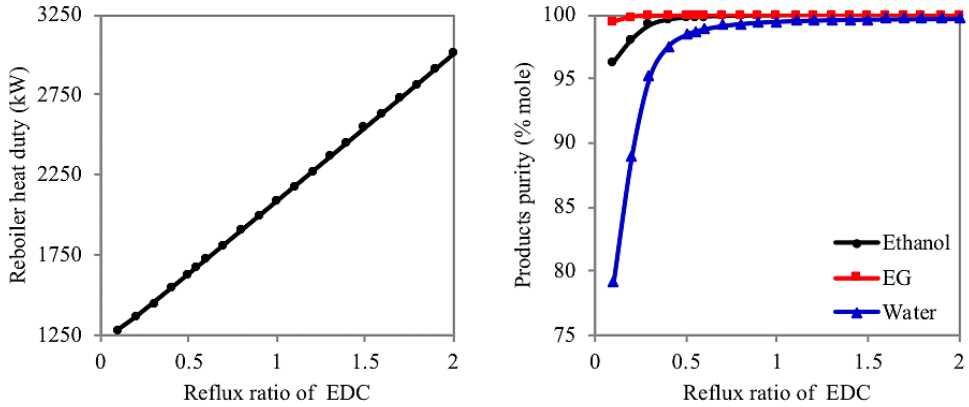

Fig. 8. The effect of reflux ratio in EDC on the purity of products (right) and reboiler heat duty (left)

4.5. Effect of the EDC feed stage

The effect of changing the feed inlet (feed stage) to EDC on the purity of the products and the heat duty of the reboiler is shown in Fig. 9. An acceptable distance between the feed and solvent inlets must be considered to allow for the absorption of water from the vapor phase by the solvent. Therefore, to perform proper separation, the feed inlet was

analyzed from the seventh stage to the side-stream stage (stage 16). From Fig. 9, it is clear that the optimal area for entering the feed, which leads to the highest purity of products and the lowest energy consumption, is between stages 11 and 13. At the top or bottom of this range, as the location of the feed is closer to the solvent or the side stream stage, proper separation does not happen. This is due to the lack of opportunity and a sufficient level for mass transfer, which, in addition to reducing the purity of ethanol and water, leads to an increase in the unit heat duty.

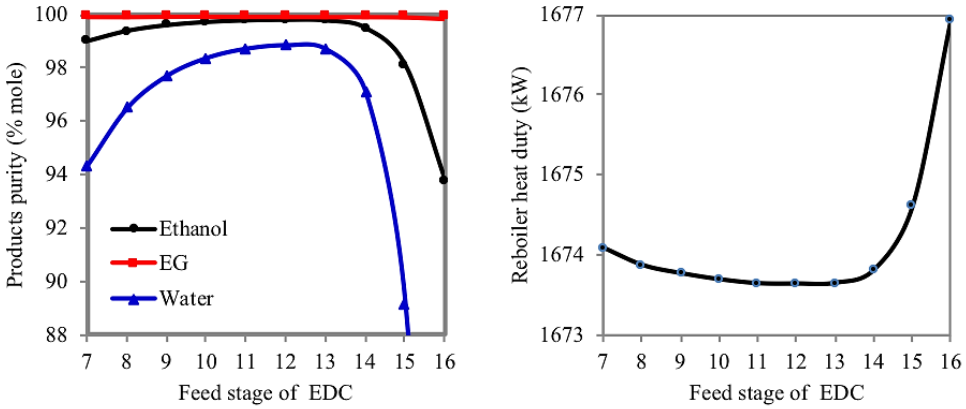

Fig. 9. The effect of the EDC feed stage on the purity of the products (right) and reboiler heat duty (left)

4.6. Effect of the EDC solvent stage

The solvent usually enters the EDC from the top trays to provide enough time to separate one of the key components of the feed. As shown in Fig. 10, with the entry of the solvent to the stages 3 or 4, the highest purity of products and the minimum heat duty of the reboiler are provided. Subsequently, as the solvent stage approaches the feed stage (step 13), due to a lack of sufficient contact time, the purity of the main products gradually decreases, and the amount of energy consumed gradually increases.

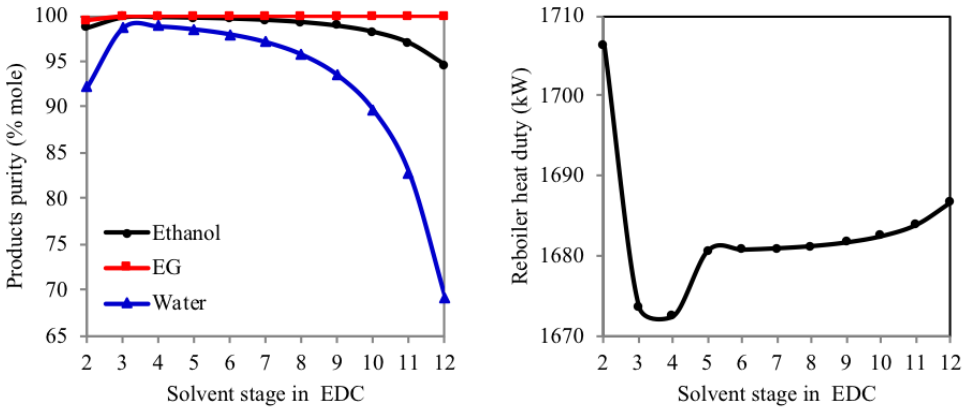

Fig. 10. The effect of the EDC solvent stage on the purity of products (right) and reboiler heat duty (left)

However, the interesting result is the entry of solvent to stage 2, which leads to a sudden increase in total heat duty and reduced purity of the products. The only reason for this phenomenon can be due to the adjacency of the solvent inlet to the reflux flow (stage 1). The reflux temperature is lower than the solvent temperature, causing a sudden decrease in the solvent temperature and, consequently, a sudden increase in heat duty.

4.7. Effect of the inlet feed temperature

In Fig. 11, the effect of temperature changes of the feed entering the EDC on the purity of the products and the heat duty of the reboiler is shown.

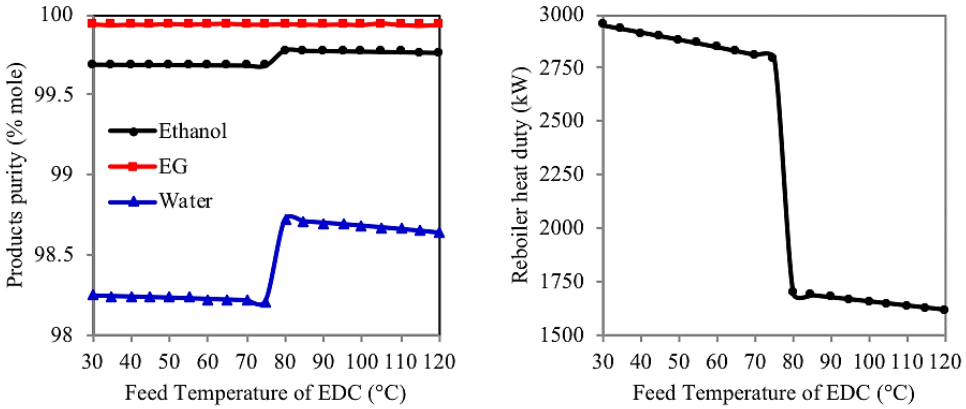

Fig. 11. The effect of the inlet feed temperature on the purity of products (right) and reboiler heat duty (left)

An interesting point in the profiles of Fig. 11 is the presence of a thermal shock and a concentration within the range of 75 to 80°C. This phenomenon is due to the presence of feed in the temperature range of its bubble and dew points[1]. In fact, increasing the inlet feed temperature reduces the reboiler's contribution to reboiling the bottoms product. As a result, the total heat duty of the unit is reduced. As noted, this effect is significant when the feed is close to its bubble or dew points (around 80°C). Therefore, a temperature of 79-85°C can be considered as the optimal temperature range of the feed. It should be noted that the change in feed temperature has a minimal effect on the purity of EG.

4.8. Effect of the inlet solvent temperature

Since the flow rate of the solvent entering the EDC is about twice the feed flow rate, any change in solvent temperature will have a significant impact on EDC performance. Increasing the temperature of the entering solvent causes a significant reduction in the reboiler's contribution to reboiling the bottoms product. Thus, in accordance with Fig. 12 (left), the heat duty of the process declines.

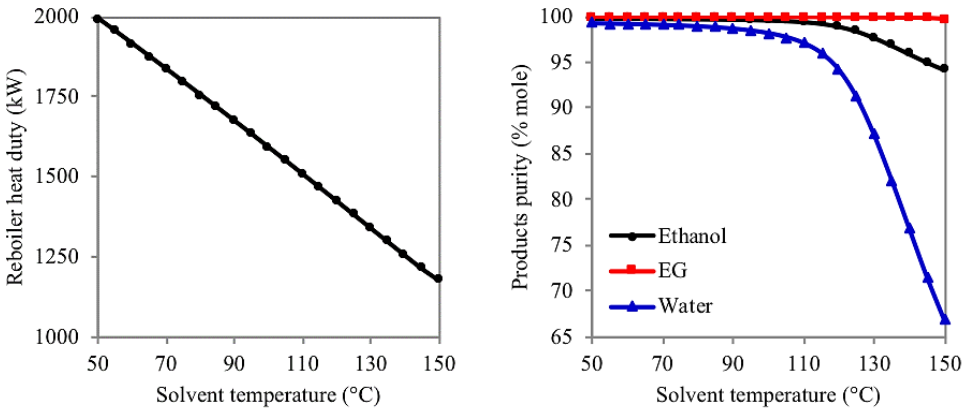

Fig. 12. The effect of the inlet solvent temperature on the purity of products (right) and reboiler heat duty (left)

[1] The bubble and dew point temperatures of the feed are 78.14°C and 78.17°C, respectively.

According to Fig. 12 (right), by increasing the solvent temperature, the purity of the main products is also reduced. In particular, from 115°C onwards, by approaching the EG boiling point (197.3°C), this decrease occurs with a steeper slope. Here, increasing the solvent temperature has a positive effect on the amount of energy consumed and a negative effect on the purity of the products; therefore, it should be considered as an intermediate value. Based on the results, the optimum temperature range for solvent entry was considered between 80°C and 115°C.

4.9. Effect of the side stream stage

The side stream should be received from the trays below the feed because the concentration of water and EG in the vapor phase is very low in the top trays. Therefore, the site of withdrawing the side stream from stage 14 (below the feed stage) to stage 23 (above the boil-up stage) was investigated. As shown in Fig. 13 (right), as the site of the withdrawal of the side stream approaches the bottom of the column, or in other words, becomes farther from the feed inlet (stage 13), a better separation is performed, and the purity of the ethanol and water products increases. In fact, this is true until the 17th stage. After that, the purity of the main products remains almost constant, except in stage 23, when the purity of the water drops. Meanwhile, the purity of EG is not dependent on the site of withdrawing the side stream, and it remains unchanged.

On the other hand, as shown in Fig. 13 (left), with withdrawing the side stream until the 20th stage, the reboiler heat duty remains roughly constant. After this stage, the heat duty increases quite sharply because, as it moves down the column, the exiting side stream has a higher temperature and more heat is removed from the column. Therefore, the reboiler must compensate for this excess heat, which results in an increase in the energy duty of the reboiler. Also, the entrance of the side stream with a higher temperature to the SAC will increase the volume of vapor in this column. As a result, the contribution of the SAC condenser increases to condense these vapors. According to the obtained results, to achieve high-purity products with the lowest energy consumption rate, the best point for withdrawing the side stream is between stages 16 and 19.

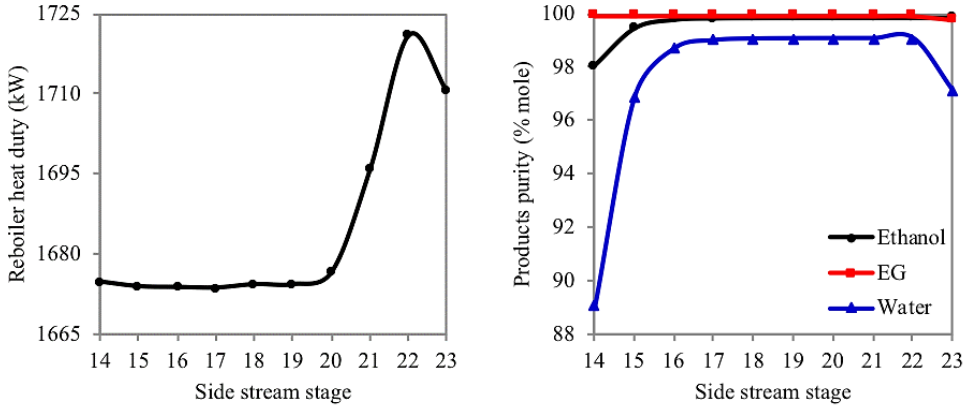

Fig. 13. The effect of the side stream stage on purity of the products (right) and reboiler heat duty (left)

4.10. Effect of the side stream flow rate

The effect of the side stream flow rate on the purity of the products and the heat duty of the reboiler is presented in Fig. 14. The flow rate of the water inside the feed is 15 kmol/h, thus, if the flow rate is lower than this value, it reduces the purity of other products. It is clear from Fig. 14 (right) that increasing the side stream causes a greater amount of ethanol to be transferred to the SAC and reduces the purity of the water received from the SAC.

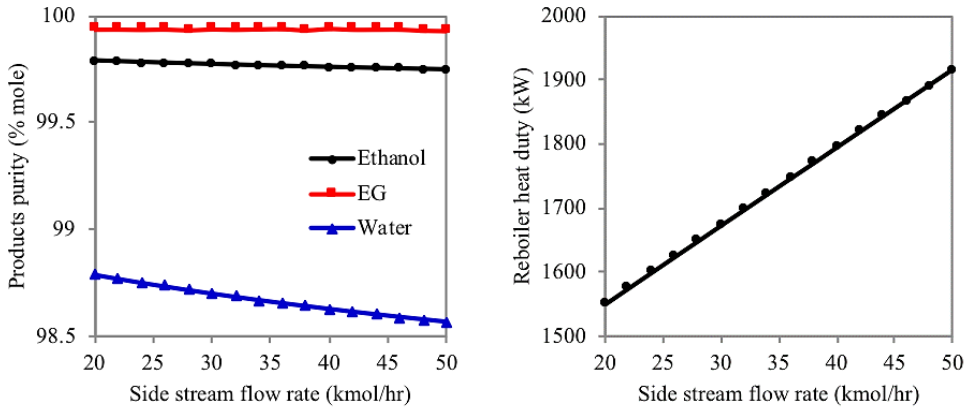

Fig. 14. The effect of side stream flow rate on the purity of the products (right) and reboiler heat duty (left)

As shown in Fig. 14 (left), with increasing side stream flow, the energy consumption duty of the unit increases dramatically. The reason for this increase is two-fold. First, the SAC condenser needs to condense large volumes of vapors, which increases the heat duty of the condenser. Second, the returning liquid flow from the SAC has a lower temperature than the liquid inside the EDC, so the cool liquid flow increases the EDC reboiler heat duty. Based on the results, to achieve high-purity products with the least energy consumption, the optimum flow rate of the side stream was considered 20kmol/h.

It should be noted that sensitivity analysis is an appropriate strategy for investigating the effect of operational variables and system design and establishing optimal process execution conditions. The results of the sensitivity analysis show clearly that feed and solvent temperatures, solvent and side stream flow rates, and reflux ratio of EDC have the highest impact on the process heat duty. Conversely, the number of EDC and SAC stages, feed, solvent, and side stream stages play a less significant role in the energy consumption of the process. On the other hand, solvent flow rate and temperature, reflux ratio of EDC, feed, solvent, and side stream stages have a significant impact on the purity of the products obtained from the process.

5. Results and discussion

In the previous section, the effect of key variables on the ethanol dehydration process was evaluated using the ED structure and SAC. After determining the optimal range of each design and operational variable separately, the sensitivity analysis was simultaneously performed on all variables in optimal ranges. In Table 9, the optimal values of the operational variables and design specifications are presented for the proposed separation pattern.

In accordance with international standards (EN 15376, ASTM D 4806), ethanol should have a purity of equal to or above 97.5-99.5 mol.% (99-99.8 wt.%) to be used as a fuel or additive [3,4]. As shown in Table 9, to obtain high-purity products, the required energy rate in the reboiler is 1270.79 kW. In this regard, the purity of ethanol, water, and EG (to return to EDC) reached 99.8%, 99% and 99.9%, respectively, which is beyond the described standards.

Uncertainty analysis was performed by perturbing optimal input operational variables (±5%), and verifying convergence limits (residuals $<10^{-6}$). The observed deviations in the outputs were less than ±2.2% (as shown in Table 10), confirming the robustness of the model and acceptable simulation accuracy.

Table 9. The optimal values of the operational parameters and design specifications of SADC

Design parameters	Value	Unit of measurement
EDC reflux ratio	0.5	kmol/kmol
Number of EDC stages	22	-
Feed stage in EDC	12	-
Solvent stage in EDC	4	-
Feed temperature	83	°C
Solvent temperature	90	°C
Drawing stage of the side stream from EDC	17	-
Returning stage of the side stream to EDC	18	-
Side stream flow rate	20	kmole/hr
SAC reflux ratio	0.788	kmol/kmol
Number of SAC stages	4	-
Ethanol flow rate in feed stream	85	kmole/hr
Water flow rate in the feed stream	15	kmole/hr
Solvent flow rate	140	kmole/hr
Reboiler heat duty in EDC	1270.79	kW
Condenser heat duty in EDC	-1388.48	kW
Condenser heat duty in SAC	-251.32	kW
EDC operating pressure	1	atm
SAC operating pressure	1	atm
Ethanol recovery	99.72	%
Water recovery	98.91	%
EG recovery	99.99	%
Ethanol purity (mole fraction)	0.998	-
Water purity (mole fraction)	0.99	-
EG Purity (mole fraction)	0.999	-

Table 10. The sensitivity of results (model outputs) per ±5% perturbation in the optimal input operational variables

Input operational variable	EG fluctuations in output (%)	Ethanol fluctuations in output (%)	Water fluctuations in output (%)	Reboiler duty fluctuations in output (%)
Feed temperature	± 0	± 0.01	± 0.03	± 0.60
Solvent temperature	± 0.01	± 0.06	± 0.35	± 2.15
Ethanol flow rate in the feed stream	± 0	± 0.51	± 1.56	± 0.07
Water flow rate in the feed stream	± 0	± 0.48	± 1.57	± 0.07
Solvent flow rate	± 0	± 0	± 0	± 0.02
Side stream flow rate	± 0	± 0	± 0.01	± 1.17
EDC reflux ratio	± 0	± 0.05	± 0.27	± 1.83
SAC reflux ratio	± 0	± 0.03	± 0.11	± 0.74
EDC & SAC operating pressure	± 0	± 0.02	± 0.08	± 1.1

Fig. 15 shows the trend of temperature variations during EDC and SAC. As shown in Fig. 15, the temperature of the stages from top to bottom of the EDC is on a roughly increasing trend. It is clear that the temperature of the first stage is close to the ethanol boiling point. In the fourth stage, the temperature of the mixture increases somewhat after entering the warm solvent. Then, until the 12th stage, which is the point of feed entry, the temperature remains almost close to the boiling point of water. The temperature of the lower feed stages increases with a fairly steep slope and holds up its uptrend until the end of the column, eventually reaching the boiling point of EG. This is due to the role of the reboiler in boiling the bottom product (EG), which leads to an increase in the temperature of the bottom feed trays. The entry of a high-temperature side stream from the bottom of the SAC leads to the highest temperature gradient at the bottom of the column. In the next stages of SAC, temperature changes occur gently, approaching the boiling point of water**.**

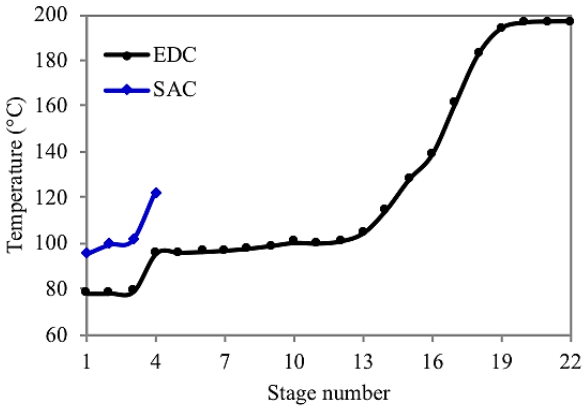

Fig. 15. The trend of temperature variations on the stages of EDC and SAC

Fig. 16 shows variation in the composition of EDC components in the liquid and vapor phases. As shown in Fig. 16 (left), the concentration of water and EG on the highest stage and the concentration of ethanol and water at the lowest stage have reached the lowest possible level. As we move down the column, ethanol goes through the liquid phase into the vapor phase, and consequently, its concentration in the liquid phase decreases. Because of the solvent entrance in stage 4, the ethanol concentration in the liquid phase suddenly decreases sharply. After that, the concentration decreases until the 16th stage with a gentle gradient. From stage 16, all the ethanol in the liquid phase evaporates, and practically water and EG remain.

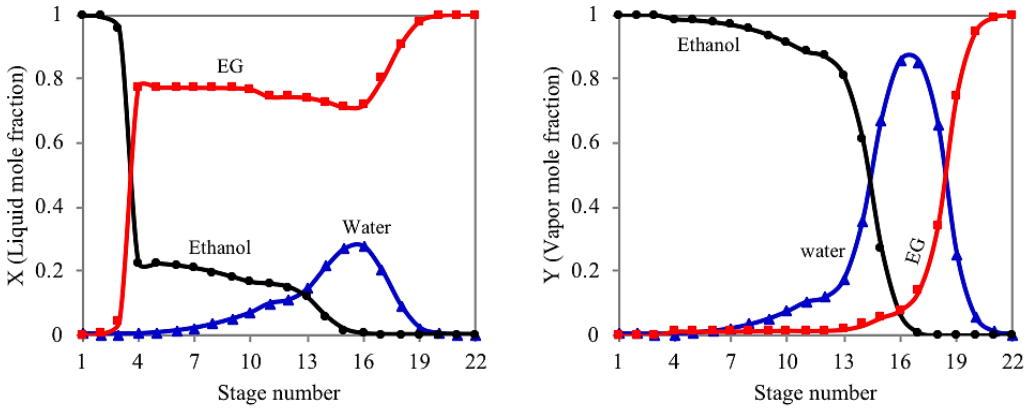

Fig. 16. The trend of variations in the composition of components in the liquid phase (left) and the vapor phase (right) on the EDC stages

In stage 4, the concentration of EG significantly increases as a result of the solvent entry, then its concentration remains constant until feed entry, but then it slightly decreases. This downward trend continues until the upper stage (step 16) of the side stream. Then, due to the return of some EG from the SAC, there was a sudden increase in the amount of it. Because of the proximity of the column temperature to the boiling point of EG, the process of increasing the concentration of this substance continues to the bottom of the column and finally reaches its maximum in the final stage**.** The concentration of water on the trays at the top of the tower is almost negligible because EG dissolves the water molecules and moves them down the column. The concentration of water starts at its lowest amount at the top of the column and reaches its maximum value at the 16th stage (above the side stream withdrawal site). The water concentration at the bottom of EDC decreases with a fairly steep gradient in the liquid phase and eventually reaches zero. This is due to the water withdrawal into the SAC and the high temperatures at the bottom of the EDC.

As shown in Fig. 16 (right), the ethanol concentration in the vapor phase is increasing in the higher stages of the side stream withdrawal (stage 17), until it reaches its maximum value in the first stage. This is due to the high volatility of ethanol in the existing temperature gradient. At the temperature gradient of the top of the tower, the concentration of water in the vapor phase is negligible. Because of the entry of the feed to stage 12, the water concentration increases, and this process continues until the side-stream withdrawal stage, reaching its maximum. Due to the outflow of water through the side-stream, its concentration in the lower trays decreases. The amount of EG in the vapor phase is very low in the upper and middle trays. This is due to the very low vapor pressure of EG compared to the other two components. Its concentration in the vapor phase increases sharply in the lower trays and reaches its maximum at the lowest stage. This is due to the high temperature generated by the reboiler.

As previously mentioned, highly purified water is extracted from SAC. Fig. 17 shows the concentration of the components in the liquid and vapor phases in the SAC. According to Fig. 17, the main changes occur in the liquid phase at lower stages and in the vapor phase at higher stages. Due to the rapid separation of EG from water in just a few stages, the size of the SAC will be small. Since the SAC temperature is close to the boiling point of water, the amount of EG in the vapor phase is negligible. Also, ethanol is present only in the vapor phase due to its low boiling point relative to other components.

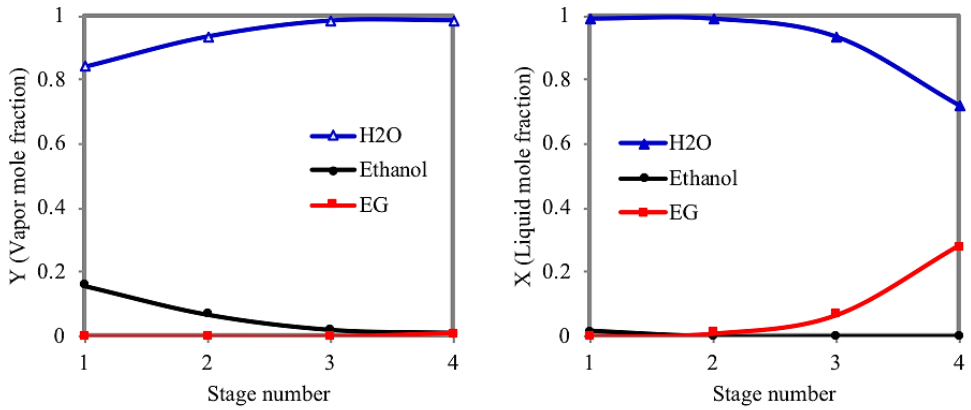

Fig. 17. The trend of variations in the composition of components in the liquid phase (left) and the vapor phase (right) on the SAC stages

5.1. Comparative view

Table 11 shows the results of comparing the SADC model with the CTC and DWC structures presented in the work of Kiss et al. [3]. The results of Table 11 indicate that the purity of products obtained through different separation structures by the ED method is approximately the same. It should be noted that providing a model that alone is capable of producing high-quality products cannot be considered an ideal model. Therefore, it is essential to consider the economic aspects of the process as well. In this comparison, what stands out most is the lower energy consumption in the SADC model compared to other separation configurations.

The energy consumption is an essential analysis for selecting the type of distillation structure when an azeotropic mixture needs an excellent separation task. As shown in Table 11, the reboiler heat duties in CTC and DWC were 2007.82 kW and 1819.52 kW, respectively, but this amount in the SADC model has reached 1270.79 kW. As a result, the reboiler heat duty in the SADC model shows a reduction of 37% and 30%, respectively, compared to the other two structures. Therefore, using the SADC structure, it is possible to prevent energy loss of 5.84 and 4.35 GW annually (during 330 working days) compared to the CTC and DWC structures, respectively.

Table 11. The comparison of product purity and heat duty required in different models of EED

Comparison parameter	Classic two-column structure [3]	Dividing-wall column [3]	The proposed model in the current paper
The recovered ethanol purity (mole fraction)	0.998	0.998	0.998
The recovered water purity (mole fraction)	0.991	0.99	0.99
The recovered EG purity (mole fraction)	0.999	0.999	0.999
Reboiler heat duty (kW)	2007.82	1819.52	1270.79
The amount of consumed solvent (kmol/hr)	190	190	140
The total number of required stages	33	36	26

In spite of energy savings, the SADC structure has one less reboiler and requires fewer stages (smaller column and associated equipment) compared to the CTC model. On the other hand, the DWC structure requires more stages than the SADC model and has a more complex configuration. In addition, the amount of solvent consumed in the SADC structure is 26.3% less than in the other two structures. Finally, it can be claimed that the SADC model requires lower investment and operating costs than the other two configurations.

Despite the advantages mentioned, some limitations of the SADC structure could be the process controllability, challenges in scale-up, and separation of mixtures with more than one azeotropic point. Also, economic feasibility, experimental validation, and environmental issues related to EG need to be carefully evaluated. All of the above can be considered as future research directions in this field.

In Table 12, the rate of specific energy consumption for high-purity ethanol production in the recent dehydration models has been compared with the present model. It is clear that the energy needed to produce one kilogram of high-purity ethanol in the current paper (0.325 $kWh/kg_{ethanol}$) is lower than all recently published articles.

Interestingly, although some researchers have used high-efficiency solvents such as ionic liquids and LTTMs, their energy consumption is not satisfactory compared to the current research. As a result, the findings of this research prove that by using a suitable separation model, there is no need to use such expensive entrainers.

Ultimately, it should be noted that because of the exceptional performance and straightforward structure of the SADC model, this design can be applied to separate other similar azeotropic mixtures.

Table 12. The comparison of the specific energy consumption rate for high-purity ethanol production in recent studies

Research work	Year	Separation structure	Entrainer	Ethanol purity (mole fraction)	Specific energy consumption ($kWh/kg_{ethanol}$)
de Figueiredo et al. [10]	2011	CTC	EG	98.73	0.403
Gil et al. [2]	2012	CTC	Glycerol	99.67	0.398
Kiss et al. [3]	2012	CTC	EG	99.85	0.513
		DWC		99.84	0.465
Vazquez-Ojeda et al. [4]	2013	CTC with pre-concentration†	EG	100	0.694
		CTC with liquid-liquid extractor†		100	1.149
Kiss et al. [11]	2014	CTC with pre-concentration*	EG	99.49	0.60
Ramos et al. [9]	2014	CTC	EG	98.73	0.404
		Single column with side stream		98.73	0.51
Figueroa et al. [7]	2015	CTC	Ionic liquid	99.76	0.844
Ma et al. [8]	2017	Distillation column with flash tank	LTTMs	99.94	0.44
Valentinyi et al. [22]	2018	CTC with pre-concentration†	EG	99.26	0.465
Miranda et al. [14]	2020	CTC	EG	99.5	0.467
Guerrero-Martin et al. [23]	2023	CTC	EG	99.62	0.445
The current research	2025	SADC	EG	99.80	0.325

† Regardless of the energy consumption in the pre-concentration stage (for the most concentrated feed used).
* Regardless of energy consumption in the pre-concentration phase.

6. Conclusion

The side-absorber distillation column is a highly capable structure for the extractive dehydration of ethanol. In this research, the simulation of the aforementioned structure was carried out based on thermodynamic principles, distillation boundaries, and residual curves. After optimizing process key factors through sensitivity analysis, the model was able to separate high-purity ethanol. This separation structure yielded products with purity exceeding defined standards (99.8% ethanol, 99% water, and 99.9 mol.% EG) and with the lowest energy consumption rate (0.325 kWh/kg ethanol) compared to similar studies in this field.

Sensitivity analysis revealed that, on the one hand, among all the factors affecting the process, feed and solvent temperatures, solvent and side-stream flow rates, and EDC reflux ratio have the greatest impact on the process heat duty. On the other hand, flow rate and temperature of the solvent, EDC reflux ratio, and the stages of feed, solvent, and side-stream play the greatest role in the purity of the products received from the process.

Among other achievements of this study can be referred to the 37% and 30% reduction in reboiler heat duty in the SADC model compared to the CTC and DWC structures. Thus, preventing energy losses of about 5.84 GW and 4.35 GW throughout the year. Also, the amount of solvent consumed in the SADC model was reduced by 26.3% compared to the other two configurations. In addition to reducing energy consumption and obtaining high-purity products, the SADC model has a simpler and smaller structure than other ethanol dehydration models. As a result, it requires lower investment and operating costs. Finally, due to the high separation potential of the model used, it can be applied to separate other azeotropic mixtures.

References

[1] Soares, R.B., Pessoa, F.L.P., Mendes, M.F., 2015. Dehydration of ethanol with different salts in a packed distillation column, Process Safety and Environmental Protection, 93, 147-153. https://doi.org/10.1016/j.psep.2014.02.012

[2] Gil, I.D., Gomez, J.M., Rodriguez, G., 2012. Control of an extractive distillation process to dehydrate ethanol using glycerol as entrainer, Computers and Chemical Engineering, 39, 129– 142. https://doi.org/10.1016/j.compchemeng.2012.01.006

[3] Kiss, A.A., Suszwalak, DJ.P.C., 2012. Enhannced bioethanol dehydration by extractive and azeotropic distillation in dividing-wall column, Separation and Purification Technology, 86, 70-78. https://doi.org/10.1016/j.seppur.2011.10.022

[4] Vazquez-Ojeda, M., Segovia-Hernandez, J.G., Hernandez, S., Hernandez-Aguirre, A., Kiss, A.A., 2013. Design and optimization of an ethanol dehydration process using stochastic methods, Separation and Purification Technology, 105, 90–97. https://doi.org/10.1016/j.seppur.2012.12.002

[5] Granjo, J.F.O., Nunes, D.S., Duarte, B.P.M., Oliveira, N.M.C., 2020. A comparison of process alternatives for energy-efficient bioethanol downstream processing, Separation and Purification Technology, 238, 116414. https://doi.org/10.1016/j.seppur.2019.116414

[6] Polyakova, M., Skiborowski, M., 2025. Next-generation pervaporation-assisted distillation: Recent advances in process intensification, Chemical Engineering and Processing - Process Intensification, 216, 110416. https://doi.org/10.1016/j.cep.2025.110416

[7] Figueroa, J.E.J., Rodrigues, M.I., Maciel, M.R.W., 2015. Sequential strategy of experimental design I: Optimization of extractive distillation process of ethanol–water using [bmim][N(CN)2] as entrainer, Chemical Engineering and Processing: Process Intensification, 93, 56–60. https://doi.org/10.1016/j.cep.2015.04.008

[8] Ma, Sh., Hou, Y., Sun, Y., Li, J., Li, Y., Sun, L., 2017. Simulation and experiment for ethanol dehydration using low transition temperature mixtures (LTTMs) as entrainers, Chemical Engineering & Processing: Process Intensification, 121, 71–80. https://doi.org/10.1016/j.cep.2017.08.009

[9] Ramos, W.B., Figueiredo, M.F. and Brito, R.P., 2014. Optimization of Extractive Distillation Process with a Single Column for Anhydrous Ethanol Production, Proceedings of the 24th European Symposium on Computer Aided Process Engineering – ESCAPE 24, Budapest, Hungary, June 15-18.

[10] de Figueiredo, M.F., Guedes, B.P., de Araujo, J.M.M., Vasconcelos, L.G.S., Brito, R.P., 2011. Optimal design of extractive distillation columns-A systematic procedure using a process simulator, Chemical Engineering Research and Design, 89 (3), 341–346. https://doi.org/10.1016/j.cherd.2010.06.011

[11] Kiss, A.A., Ignat, R.M. and Bildea, C.S., 2014. Optimal Extractive Distillation Process for Bioethanol Dehydration, Proceedings of the 24th European Symposium on Computer Aided Process Engineering – ESCAPE 24, Budapest, Hungary, June 15-18.

[12] Alvarez, V.H., Alijo, P., Serrao, D., Filho, R.M., Aznar, M., Mattedi, S., 2009. Production of Anhydrous Ethanol by Extractive Distillation of Diluted Alcoholic Solutions with Ionic Liquids, Computer Aided Chemical Engineering, 27, 1137-1142. https://doi.org/10.1016/S1570-7946(09)70410-9

[13] Zhu, Zh., Ri, Y., Li, M., Jia, H., Wang, Y., Wang, Y., 2016. Extractive distillation for ethanol dehydration using imidazolium-based ionic liquids as solvents, Chemical Engineering and Processing: Process Intensification, 109, 190–198. https://doi.org/10.1016/j.cep.2016.09.009

[14] Miranda, N.T., Maciel Filho, R., Wolf Maciel, M.R., 2020. Comparison of Complete Extractive and Azeotropic Distillation Processes for Anhydrous Ethanol Production Using Aspen Plus™ Simulator, Chemical Engineering Transactions, 80, 43-48. https://doi.org/10.3303/CET2080008

[15] Imad, M., Castro-Muñoz, R., 2023. Ongoing Progress on Pervaporation Membranes for Ethanol Separation, Membranes, 13(10), 848. https://doi.org/10.3390/membranes13100848

[16] An, Y., Li, W., Li, Y., Huang, Sh., Ma, J., Shen, Ch., Xu, Ch., 2015. Design/Optimization of Energy-Saving Extractive Distillation Process by Combining Preconcentration Column and Extractive Distillation Column, Chemical Engineering Science, 135, 166-178. https://doi.org/10.1016/j.ces.2015.05.003

[17] Quijada-Maldonado, E., Aelmans, T.A.M., Meindersma, G.W., de Haan, A.B., 2013. Pilot plant validation of a rate-based extractive distillation model for water–ethanol separation with the ionic liquid [emim][DCA] as solvent, Chemical Engineering Journal, 223, 287–297. https://doi.org/10.1016/j.cej.2013.02.111

[18] Quijada-Maldonado, E., Meindersma, G.W., de Haan, A.B., 2014. Ionic liquid effects on mass transfer efficiency in extractive distillationof water–ethanol mixtures, Computers and Chemical Engineering, 71, 210–219. https://doi.org/10.1016/j.compchemeng.2014.08.002

[19] Kong, J., Liu, W., Fu, Y., Zhang, X., Li, Y., Li, J., Sun, L., 2025. Optimization of the process for separating ethylene glycol and 1,2-butanediol using reactive distillation-assisted separation based on a parallel stochastic algorithm framework, Separation and Purification Technology, 354 (2), 128732. https://doi.org/10.1016/j.seppur.2024.128732

[20] Shuguang Xiang, Lili Wang, Yinglong Wang, Rongshan Bi, Li Xia, Xiaoyan Sun, 2021. Exploration of gradient energy-saving separation processes for ethylene glycol mixtures based on energy, exergy, environment, and economic analyses, 279, 119787. https://doi.org/10.1016/j.seppur.2021.119787

[21] Kiss, A.A. and Suszwalak, DJ.P.C., 2012. Efficient bioethanol dehydration in azeotropic and extractive dividing-wall columns, Proceedings of the 20th International Congress of Chemical and Process CHISA 2012, Prague, Czech Republic, August 25-29.

[22] Valentinyi, N., Marton, G., Toth, A., Haaz, E., Andre, A., Mizsey, P., 2018. Investigation of process alternatives for the separation of ethanol, n-butanol and water ternary mixture, Chemical Engineering Transactions, 69, 607-612. https://doi.org/10.3303/CET1869102

[23] Guerrero-Martin, C.A., Fernández-Ramírez, J.S., Arturo-Calvache, J.E., Milquez-Sanabria, H.A., da Silva Fernandes, F.A., Costa Gomes, V.J., Lima e Silva, W., Valente Duarte, E.D., Guerrero-Martin, L.E., Lucas, E.F., 2023. Exergy Load Distribution Analysis Applied to the Dehydration of Ethanol by Extractive Distillation, Energies, MDPI, 16(8), 1-14. https://doi.org/10.3390/en16083502

[24] García-Ventura, U.M., Barroso-Muñoz, F.O., Hernández, S., 2016. Castro-Montoya, A.J., Experimental study of the production of high purity ethanol using a semi-continuous extractive batch dividing wall distillation column, Chemical Engineering and Processing: Process Intensification, 108, 74–77. https://doi.org/10.1016/j.cep.2016.07.014

[25] Alcántara-Avila, J.R., Kano, M., Hasebe, S., 2012. Environmental and economic optimization of distillation structures to produce anhydrous ethanol, Computer Aided Chemical Engineering, 30, 712-716. https://doi.org/10.1016/B978-0-444-59520-1.50001-4

[26] Shirsat, S.P., Dawande, Sh.D. , Kakade, S.S., 2013. Simulation and optimization of extractive distillation sequence with pre-separator for the ethanol dehydration using n-butyl propionate, Korean Journal of Chemical Engineering, 30, 2163-2169. https://doi.org/10.1007/s11814-013-0175-8

[27] Thein, T.Z., Htway, W.M., Tun, W.E.E., 2018. Dehydration of Aqueous Ethanol Mixtures by Extractive Distillation, International Journal of Science and Engineering Applications, 7(8), 162-165. https://doi.org/10.1021/ba-1972-0115.ch001

[28] Ramírez-Corona, N., Schramm-Flores, A., Reyes-Lombardo, S., Jiménez-Gutiérrez, A., 2019. Effect of ionic liquids as entrainers on the dynamic behavior of ethanol-water extractive columns, BMC Chemical Engineering, 1, 1-11. https://doi.org/10.1186/s42480-019-0023-7

[29] http://www.ddbst.com/en/EED/VLE/VLEindex.php